

DUST FORMATION AND He II λ 4686 EMISSION IN THE DENSE SHELL OF THE PECULIAR TYPE Ib SUPERNOVA 2006jc

NATHAN SMITH, RYAN J. FOLEY, & ALEXEI V. FILIPPENKO
Department of Astronomy, University of California, Berkeley, CA 94720-3411

Draft version September 12, 2018

ABSTRACT

We present evidence for the formation of dust grains in an unusual Type Ib supernova (SN) based on late-time spectra of SN 2006jc. The progenitor suffered an outburst qualitatively similar to those of luminous blue variables (LBVs) just 2 yr prior to the SN, and we propose that the dust formation is a consequence of the SN blast wave overtaking that LBV-like shell. The key evidence for dust formation is (a) the appearance of a red/near-infrared continuum emission source that can be fit by $T \approx 1600$ K graphite grains, and (b) fading of the redshifted sides of intermediate-width He I emission lines, yielding progressively more asymmetric blueshifted lines as dust obscures receding material. This provides the strongest case yet for dust formation in any SN Ib/c. Both developments occurred between 51 and 75 d after peak brightness, while the few other SNe observed to form dust did so after a few hundred days. Geometric considerations indicate that dust formed in the dense swept-up shell between the forward and reverse shocks, and not in the freely expanding SN ejecta. The rapid cooling leading to dust formation may have been aided by extremely high shell densities of 10^{10} cm^{-3} , indicated by He I line ratios. The brief epoch of dust formation is accompanied by He II λ 4686 emission and enhanced X-ray emission, suggesting a common link. These clues suggest that the unusual dust formation in this object was not attributable to properties of the SN itself, but instead — like most peculiarities of SN 2006jc — was a consequence of interaction with the dense environment created by an LBV-like eruption 2 yr before the SN.

Subject headings: dust, extinction — stars: mass loss — stars: winds, outflows — stars: Wolf-Rayet — supernovae: individual (SN 2006jc)

1. INTRODUCTION

Supernova (SN) 2006jc is a peculiar Type Ib event that challenges our understanding of the late-time evolution of massive stars in several important ways. It is one of only three known SNe Ib/c (see Filippenko 1997 for a review of supernova spectral types) that exhibit strong and relatively narrow (widths of $\sim 10^3 \text{ km s}^{-1}$; hereafter referred to as “intermediate width”) emission lines of He I in their optical spectra (Foley et al. 2007; Pastorello et al. 2007) — the other two known examples being SN 1999cq (Matheson et al. 2000) and SN 2002ao (Foley et al. 2007). SNe Ib/c probably mark the deaths of Wolf-Rayet (WR) stars, but the intermediate-width He I lines in these three objects indicate much denser circumstellar material (CSM) than that around all other SNe Ib/c, and similarly, inferred progenitor mass-loss rates much higher than those typically observed in WR stars (Crowther 2007). X-rays detected from SN 2006jc also imply strong CSM interaction (Immler et al. 2008).

What may turn out to be the most important aspect of SN 2006jc, unique among all SNe observed so far, is that the progenitor star was observed to have suffered a giant outburst qualitatively similar to those of luminous blue variables (LBVs) just 2 yr before being discovered as a SN (Nakano et al. 2006; Pastorello et al. 2007). These outbursts, sometimes called “supernova impostors” when they are seen in other galaxies, are thought to be analogous to the 19th-century eruption of η Carinae, which ejected $\sim 10 M_{\odot}$ within about a decade (Smith et al. 2003). The best-known extragalactic example is SN 1961V in NGC 1058 (e.g., Goodrich et al. 1989;

Filippenko et al. 1995; Van Dyk et al. 2002).

LBVs are usually presumed to be stars in transition from core-H burning to He burning, so they should not explode as SNe for another few hundred thousand years. However, there is mounting evidence to the contrary, that some LBVs — or related H-rich stars with similar eruptive mass loss — defy expectations of stellar evolution models and might in fact explode as SNe (Smith & Owocki 2006; Kotak & Vink 2006; Gal-Yam et al. 2007; Smith 2007; Smith et al. 2007). The apparent magnitude of the transient event 2 yr before SN 2006jc was consistent with one of these giant LBV eruptions, but to see one from a WR star is highly unexpected, as noted by Foley et al. (2007) and Pastorello et al. (2007).

Stellar evolution theory currently makes no prediction that the LBV-like instability should continue to play a role through the start of the WR phase¹, but there are some observational indications that the two phenomena may be closely related (see Smith & Conti 2008). It is an observational fact that giant LBV eruptions can remove large amounts of mass (of order $10 M_{\odot}$) in short bursts that last a decade, occurring multiple times, and that these sudden mass ejections may therefore be the dominant mechanism responsible for shedding a star’s H-rich envelope to produce a WR star (Smith & Owocki 2006). In retrospect, perhaps it should not be surprising, then, if the instability responsible for making a WR star persists into the early WR phase itself.

¹ To be fair, though, stellar evolution theory makes no clear prediction of the LBV instability during the LBV phase either, since the mechanism is not understood.

A few well-known examples point in this direction. Among the more luminous and most exemplary of the LBVs are AG Carinae in our Galaxy and R 127 in the Large Magellanic Cloud. Both of these LBVs are surrounded by massive ring nebulae (Stahl 1987), and both have been classified as Ofpe/WN9 stars in their hot quiescent phases when they were not exhibiting the LBV behavior (Stahl 1986; Stahl et al. 1983). The Ofpe/WN9 stars (Bohannon & Walborn, 1989; Crowther et al. 1995; alternatively called WN11) are probably not core-He burning WR stars, and many have never been observed to undergo an LBV eruption; they are still H-rich, but they are thought to represent one of the transitional phases between O stars and WR stars.

Another intriguing object is the eclipsing binary HD 5980 (Koenigsberger 2004), the most luminous star known in the Small Magellanic Cloud. It consists of two stars with WN-like spectra, one of which suffered a brief LBV-like outburst in 1994 (Barbá et al. 1995; Koenigsberger 2004). The outburst was shorter in duration, less luminous, and ejected far less mass than the eruptions of η Car or SN 1961V, but it had properties in common with some LBV outbursts. The erupting star was H rich (Koenigsberger 2004; Koenigsberger et al. 2000; Moffat et al. 1998), so although its spectrum showed WN-like features, it too has not yet shed its H envelope to become a *bona fide* WR star and is probably instead a transition object (Smith & Conti 2008). Nevertheless, these connections may be relevant to SN 2006jc after all, which had weak H α emission in its spectrum (Foley et al. 2007), although still H poor.

In a previous paper (Foley et al. 2007, hereafter Paper I) we presented and discussed our early-time optical spectra and light curves of SN 2006jc. The most important result for our purposes here is that the unusual intermediate-width He I lines of SN 2006jc are probably produced through ejecta interacting with its dense CSM that was created by the LBV-like eruption observed 2 yr before the SN. The implications for stellar evolution are quite provocative, as noted above, because this is the first case of an LBV-like eruption in a H-poor star. Pastorello et al. (2007) reached a similar conclusion independently, although they also propose that a classical LBV outburst may have occurred in a companion star in a binary system instead of the same star that died to make SN 2006jc. However, the observed emission from the CSM of SN 2006jc requires that the companion's LBV outburst would need to have been H poor as well, making this scenario doubtful.

Here we explore the influence of this dense CSM created in the LBV-style outburst from the perspective of evidence for the rapid formation of dust grains in SN 2006jc. Based on near-infrared (near-IR) broadband photometry, Arkharov et al. (2006) found that SN 2006jc was rebrightening in the H and K bands in late-November through early-December 2006, and they conjectured that this unusual outburst was likely to have “some kind of relation with dust.” Whether the dust was pre-existing or formed in the SN is not obvious from the near-IR photometry alone.

Grain formation would be very unusual for SNe Ib/c; the Type Ib SN 1990I is the only previous case where dust formation is thought to have occurred (Elmhamdi et al. 2004). In fact, clear evidence for dust formation in SNe

has been elusive for any type of SN, even though the idea that SNe could form dust was postulated long ago (e.g., Cernuschi, Marsicano, & Codina 1967; Hoyle & Wickramasinghe 1970). Observations of SN 1979C (Merrill 1980) and SN 1980K (Dwek et al. 1983) showed suggestive evidence for dust formation, but SN 1987A provided the first well-established case. SN 1987A showed an IR excess, a simultaneous decrease in its optical light, and a systematic blueshift in its broad emission lines formed in the SN ejecta (Danziger et al. 1989; Lucy et al. 1989; Gehrz & Ney 1989; Wooden et al. 1993; Colgan et al. 1994; Wang et al. 1996; Moseley et al. 1989; Dwek et al. 1992). Two more-recent cases providing evidence for dust formation are SN 1999em (Elmhamdi et al. 2003) and SN 2003gd (Sugerman et al. 2006), although Meikle et al. (2007) found that the mass of dust formed in SN 2003gd was very small. All three of these were Type II explosions where the dust formed in the SN ejecta. Dust in SN remnants (SNRs) is usually dominated by swept-up interstellar or circumstellar dust. A rare exception is the Crab Nebula, where $\lesssim 0.01 M_{\odot}$ of dust is seen (Temim et al. 2006).

An observed near-IR excess alone is not sufficient evidence for dust formation. Unlike the case of classical novae, where the temporal development of the observed excess shows clear evidence for new grain formation in the ejecta (e.g., Gehrz 1988), in SNe the observed IR excess is often attributed to a light echo (Dwek 1983; Emmering & Chevalier 1988; Bode & Evans 1980). This arises when light from the SN illuminates and heats pre-existing dust in the CSM.

In this paper we present evidence from optical spectra that the near-IR rebrightening of SN 2006jc noted first by Arkharov et al. (2006) is indeed caused by dust *formation*, and not an IR light echo. Our key result is that the dust formation in SN 2006jc is directly linked to its unusually dense environment, and that dust formed in the dense post-shock shell rather than within freely expanding SN ejecta. SN 2006jc is the first clear example of a SN forming dust in this way.

In §2 we present new late-time optical spectra of SN 2006jc that were obtained after those published in Paper I, and in §3 and §4 we discuss two independent lines of evidence that dust has formed. In §5 we give reasons why the near-IR excess in SN 2006jc is probably *not* the result of pre-existing circumstellar dust heated by the SN. In §6 we consider the geometry and location of this dust, and in §7 we summarize our key results.

2. NEW OPTICAL SPECTRA OF SN 2006jc

In Paper I, we presented and discussed early-time low-resolution and moderate-resolution spectra of SN 2006jc up to day 44 after the time when photometric monitoring began (near the B -band peak). These were obtained with the Kast spectrograph (Miller & Stone 1993) on the Lick Observatory 3-m Shane reflector, as well as with the LRIS (Oke et al. 1995) and DEIMOS (Faber et al. 2003) spectrographs mounted on the 10-m Keck I and II telescopes, respectively. Here we present additional optical spectra obtained at later times using the same observational setups and data-reduction techniques (see Paper I for further details). The additional spectra discussed here were obtained on UT dates of 2006 December 1.4 (day 51; Lick Kast), 2006 December 25.5 (day 75; Keck

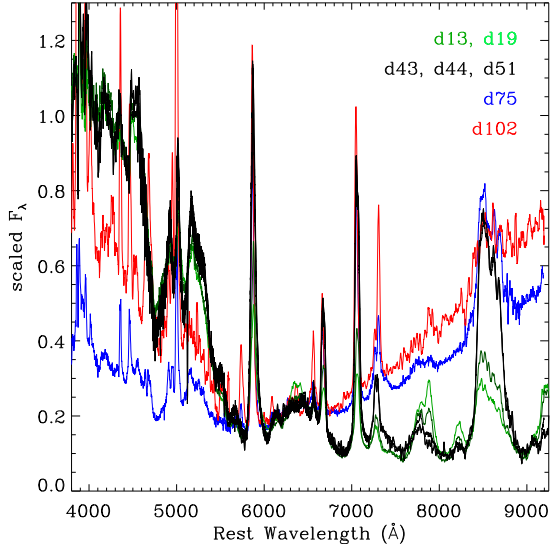


FIG. 1.— Optical spectra of SN 2006jc from early times (two weeks after explosion) until late times, scaled to highlight changes in the relative continuum shape. By late-December 2006 (day 75) through late-January 2007 (day 102), SN 2006jc showed a pronounced red continuum that had not been present before. Its strength was comparable to that of the blue emission, creating a “U”-like shape in the optical continuum. The spectra were normalized near 6400 Å.

LRIS), 2007 January 21.5 (day 102; Keck LRIS), and 2007 February 16.5 (day 128; Keck DEIMOS).

3. EVIDENCE FOR DUST: THE RED CONTINUUM

3.1. Changes in the Continuum Shape

Figure 1 shows optical spectra obtained during the first ~ 100 d of SN 2006jc, with the flux scaled to highlight changes in the relative continuum shape (normalized roughly to the R -band flux). As noted in Paper I, there are pronounced changes with time in the relative strengths of intermediate-width features like the He I lines, as well as the broad features emitted by the SN ejecta such as the Ca II near-IR triplet and O I $\lambda 7774$.

Setting these contributions from specific lines aside, though, it is stunning how little the underlying shape of the optical spectrum changes at early times. Until at least ~ 50 d (green and black in Fig. 1), there is essentially *no change* in the shape of the continuum to within a few percent, despite the rapid fading of the SN by a factor of ~ 15 during the same time interval. The photometric $B - R$ color stays nearly constant during this time as well (Paper I). The spectrum persistently shows a flat, weak, red continuum, but shortward of ~ 5500 Å, the continuum abruptly jumps upward to produce a strong blue/near-UV continuum. Even the detailed undulations of this blue “continuum” did not change by more than a few percent during the first ~ 50 d (Fig. 1). This step blue continuum remains puzzling, but was also seen in the Type II_n SN 1998S (Leonard et al. 2000); in Paper I we suggested that it may be caused by many blended Fe lines, perhaps due to fluorescence (broadly construed to include UV or collisional excitation). We noted that the two other SNe Ib/c with strong, intermediate-width He I lines (SNe 2002ao and 1999cq) show similar blue continua, although not as strong as in SN 2006jc, perhaps due to line-of-sight reddening from dust.

The continuum shape of SN 2006jc then took a bizarre

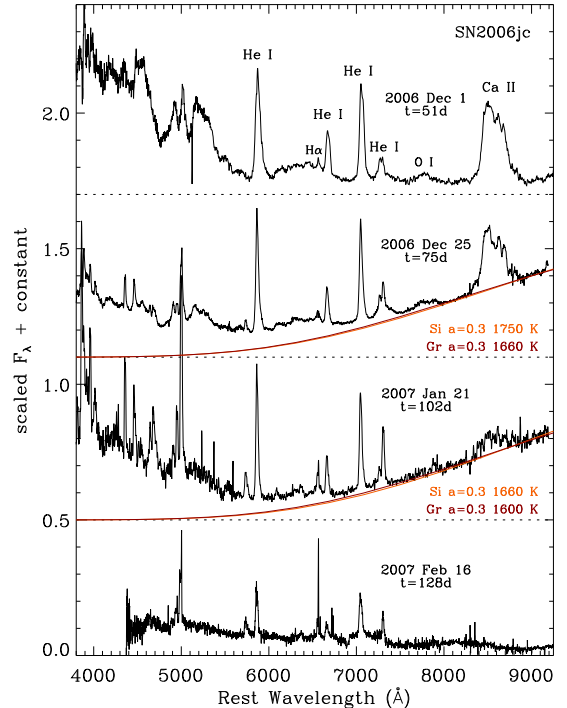


FIG. 2.— Late-time optical spectra of SN 2006jc from Figure 1 but plotted individually. The pronounced red continuum that was present in late-December 2006 through January 2007 had not been present before, and disappeared by mid-February 2007. (We suspect that our final spectrum on day 128 may be contaminated by an underlying star cluster and H II region; prominent, very narrow H α emission is present.) At the epochs when the strong red continuum is present, red and orange curves show models for emission from graphite and silicate grains, respectively, at the temperatures indicated. The curves shown here use emissivities from silicate and graphite grains of radius $a = 0.3 \mu\text{m}$ from Draine & Lee (1984), but the results do not depend strongly on assumed grain radius as long as a is less than $\sim 1 \mu\text{m}$.

turn sometime in mid-December 2006. By Dec. 25 (day 75; blue in Fig. 1) the continuum looked completely different. The blue-wavelength continuum was still present, although it was not as steep, having dropped by almost a factor of three relative to 6500 Å. The most striking change was at red and near-IR wavelengths, where SN 2006jc developed a strong continuum component not present in any earlier spectra. With the spectrum rising into the blue *and* rising sharply into the near-IR, the optical continuum took on a “U”-like shape that has not been documented as clearly in any other SN. This “U”-shaped continuum was still present a month later in late-January 2007 (day 102; red in Fig. 1).

Figure 2 shows our late-time optical spectra of SN 2006jc, with the last four epochs plotted individually. The first epoch at day 51 is essentially identical to the day 43/44 spectra that were the latest ones discussed in Paper I. The spectra at days 75 and 102 clearly show the new near-IR excess emission that subsequently disappeared by day 128.

The most plausible explanation for this transient red/near-IR continuum emission is that it is caused by hot dust – either newly formed hot dust, or pre-existing dust in the CSM that is heated by energy input from the SN. We will return to these options later. For now, the purpose of Figure 2 is simply to illustrate that hot dust

can account for the transient red continuum shape.

Although the shape of the red continuum excess can be approximately fit by a ~ 2000 K Planck function, optically thin emitting dust grains will have wavelength-dependent emissivity. As long as the grains are not larger than about $a = 1 \mu\text{m}$, the dust will typically have emissivity proportional to λ^β , with $-2 \lesssim \beta \lesssim -1$. The red and orange curves in Figure 2 are plotted adopting the emissivities of graphite and astronomical silicate, respectively, both with $a = 0.3 \mu\text{m}$ (Draine & Lee 1984). They are nearly identical, meaning that from the emission at these wavelengths alone, we are unable to directly constrain the grain chemistry. However, the high temperature needed to produce the red continuum shape gives an important clue. With these emissivities, the grain temperatures are around 1600 K for graphite particles, or slightly warmer for silicates (Fig. 2). Standard theory for carbon condensation (Clayton 1979) and models of dust formation in SN ejecta (Todini & Ferrara 2001) predict that nucleation starts at $T \approx 1800$ K for carbon grains, while silicates require lower temperatures of 1000–1200 K, as typically seen in novae (Gehrz 1988). Thus, Figure 2 is compatible with the notion that this red emission arises from freshly synthesized, amorphous carbon dust in SN 2006jc, while the high temperatures seem problematic for silicates.

3.2. Luminosity and Mass of the Hot Dust

Figure 3 shows the same data and the same silicate and graphite dust models for day 75 from Figure 2, but plotted as λF_λ on an absolute flux scale with a broader wavelength range. We would normally use our optical photometry of SN 2006jc to directly check our absolute flux calibration of the spectrum, but our optical photometry of SN 2006jc ended just over a week before the day 75 spectrum (black in Fig. 3) was obtained. Extrapolating our light curve using the late-time decline rate of 0.066 mag d^{-1} (Paper I), we estimate SN 2006jc to have $R = 18.8$ mag on 2006 Dec. 25. Using this as a guide, we derive a continuum flux at 6900 \AA of $5.3 \times 10^{-17} \text{ erg s}^{-1} \text{ cm}^{-2} \text{ \AA}^{-1}$. The relative fluxes should be reliable at the 5% level. Figure 3 includes an earlier spectrum on day 51 (green) where no evidence of dust is seen, and broad-band *BVRJHK* photometry from 4–5 d later, showing early signs of the IR excess. The *BVRI* photometry is from our database (see Paper I) and the *JHK* measurements are from Arkharov et al. (2006). We include error bars for all of the broad-band photometry, but the quoted uncertainty of 0.03 mag in the *JHK* bands from Arkharov et al. is smaller than the plotting symbols.

Photometry at longer IR wavelengths may constrain the dust emission and chemistry better than our optical spectra, since we expect λF_λ values of the hot dust to peak in the *H* and *K* bands or at even longer wavelengths. The graphite and silicate models in Figure 3 predict fluxes extrapolated in the *H* and *K* bands that differ by 0.2 and 0.4 mag, respectively, with the weaker fluxes corresponding to graphite. These differences are large enough that near-IR broad-band photometry should be able to constrain the dust chemistry by comparison with Figure 3. However, Figure 3 should not necessarily be regarded as a *prediction* of the total IR emission, but rather, only an extrapolation of emission from the hottest

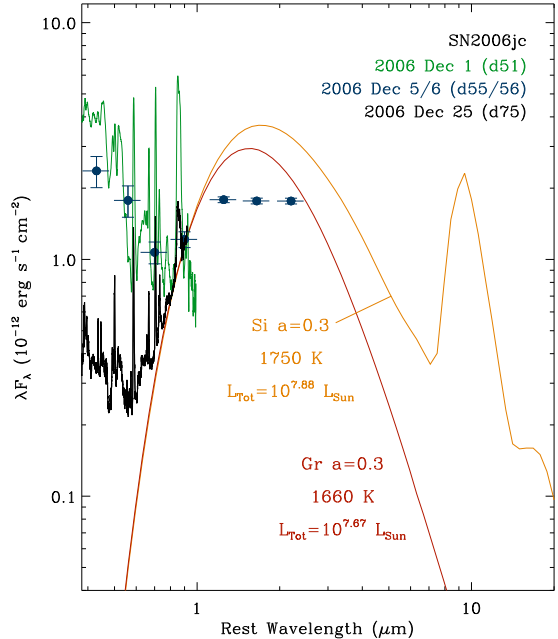


FIG. 3.— The spectrum and dust models for 2006 Dec. 25 from Figure 2 extrapolated into the IR. The observed spectra were flux calibrated as noted in the text, and the models show predicted values of λF_λ for the silicate (orange) and graphite (red) grains from Figure 2. The integrated luminosity of each dust component is noted as well. The black spectrum is from day 75 when the IR emission appears to have peaked. The day 51 spectrum from Figure 2 is shown in green, and the broad-band *BVRJHK* spectral energy distribution from a few days later is shown in blue (see text).

newly formed dust. It should therefore be regarded as a lower limit to the near/mid-IR emission under each assumption for the grain composition. If our preferred scenario (see §6) is correct, we actually expect cooler dust to “pile up” and give rise to greater IR excess emission at longer mid-IR wavelengths, above the flux indicated by the curves in Figure 3.

The bolometric IR luminosity of the new dust that appears to have reached its peak emission on Christmas Day 2006 (Fig. 3) is roughly $5 \times 10^7 L_\odot$ for graphite or $8 \times 10^7 L_\odot$ for silicates (the difference is due to the different wavelength-dependent emissivities of the two materials). This IR dust luminosity is several times greater than the integrated optical luminosity of the SN itself at the same epoch, estimated as follows. If we extrapolate the late-time decline rate for the light curve in Paper I, as noted above, and we assume a distance modulus of 31.8 mag for the host galaxy UGC 4904, we find that SN 2006jc should have rough absolute *BVRI* magnitudes of -12.26 , -12.48 , -12.98 , and -13.83 , respectively, on day 75. This relative photometry should also be accurate at the 5% level. If we adopt plausible bolometric corrections of -0.74 , -0.09 , -0.32 , and -0.66 mag for these filters (see Paper I), we find an average bolometric magnitude of -12.85 , or an intrinsic luminosity of roughly $10^7 L_\odot$. The fact that this is several times less than the integrated dust luminosity agrees with the general impression of the λF_λ plot in Figure 3, where the blue/near-UV luminosity on day 75 is far below the peak of the IR emission. This luminosity difference supports the idea (see §6) that the dust does not reside within the SN ejecta where it would be heated continually by the

central engine of ^{56}Ni decay, because there is not enough radiative luminosity to heat the dust. Instead, the IR emission draws its energy supply from the dense, post-shock radiative cooling zone.

The bolometric IR luminosity of the dust component can also be used to estimate the mass of hot emitting dust; below we take graphite grains as an example. As long as the grains are small ($a \lesssim 0.3 \mu\text{m}$), the mass of emitting dust can be expressed independent of the assumed grain radius and emissivity as

$$M_d = [(100\rho)/(3\sigma T_d^6)] \times L_d,$$

where $\rho = 2.25 \text{ g cm}^{-3}$ is the assumed density of graphite grains, σ is the Stefan-Boltzmann constant, T_d is the observed dust temperature of $\sim 1600 \text{ K}$, and L_d is the total dust luminosity (see Smith & Gehrz 2005; Gehrz 1999; Gilman 1974). From the observed dust luminosity and temperature, we find a dust mass of $\sim 6 \times 10^{-6} M_\odot$ present on day 75. This is only the mass of the very hottest emitting dust present at the time of the observations; it is not the total mass of dust formed by SN 2006jc, because this dust will cool rapidly and will be continuously replaced by additional hot dust as long as the dust-formation epoch continues. This can only be regarded as a minimum mass, since we are insensitive to cooler dust emitting at longer IR wavelengths.

The total (i.e., cumulative) mass of dust produced as the shock sweeps all the way through the dense shell is this instantaneous value multiplied by $\Delta t/t_{\text{cool}}$, where Δt is the observed duration of dust formation (roughly 1–2 months), and t_{cool} is the cooling timescale of the dust in the dense post-shock gas. If the gas-grain cooling time is short (less than, say, 1 hr), as we might expect for the observed temperatures and very high gas densities in the post-shock shell (see Burke & Hollenbach 1983), then the total dust mass produced by SN 2006jc could be as high as 1% of a solar mass or more (and hence, the mass ejected in the LBV-like event may have been as high as $1 M_\odot$ for a normal gas:dust ratio). This is only an order of magnitude estimate, of course, because of the large uncertainty in the value of t_{cool} . Over time, we would predict the following approximate behavior: As dust grains continued to form over the 1–2 months when we detect the hot near-IR excess, a range of dust temperatures will be seen. The hottest newly formed dust will continue to be seen at $\sim 1600 \text{ K}$, while dust that has cooled will “pile up” at progressively lower temperatures, causing the flux to rise at longer IR wavelengths. After active dust formation stops (sometime before day 128) this range of dust temperatures will continue to cool as the dust expands and the SN fades, and its emission will shift into the mid-IR.

Other changes also occurred in the spectrum of SN 2006jc at the same time as the dust formation, supporting the view that a substantial amount of new dust formed. Between days 50 and 75, the blue continuum was seen to change its shape for the first time, having faded strongly compared to the *R*-band flux (Fig. 1). Moreover, starting at around day 50, the visual light curve of SN 2006jc began to decline faster than the ^{56}Co decay rate (Paper I). Similarly, both the Ca II near-IR triplet and O I $\lambda 7774$ faded away as the red continuum excess grew stronger. We speculate that the fading of the blue

continuum and the fading of these lines formed in the SN ejecta are both a consequence of obscuration by the newly synthesized dust. We discuss the possible effects of extinction by dust in the next section.

The red excess emission seems to have disappeared by mid-February 2007 (day 128), although the SN was so faint by this time that our spectra may be contaminated by light from an underlying star cluster and H II region. This rapid disappearance of the dust emission is unlike the case in SNe IIn with dust, where the IR excess typically lasts for years (Gerardy et al. 2002). Did the red dust emission in SN 2006jc vanish because the grains were destroyed or because they cooled? We offer a possible answer in the following section.

4. EVIDENCE FOR DUST: CHANGING LINE PROFILES

Another type of observation at optical wavelengths that has been interpreted as evidence for dust formation in SN ejecta is the development of asymmetric line profiles with a net blueshift as the ejecta expand and cool. Specifically, as dust grains condense in the SN ejecta, one would expect this dust to obscure progressively more emission from the far side of the object. This should cause optically thin emission-line profiles to become more asymmetric in shape and to shift the bulk of their emission toward bluer velocities as emission from the redshifted gas is blocked. This effect has been documented in several SNe II, most notably in SN 1987A (Danziger et al. 1989; Lucy et al. 1989; Colgan et al. 1994; Wang et al. 1996), indicating the formation of new dust in the ejecta at $\sim 500 \text{ d}$ after explosion.

Whether this effect is common in SNe Ib/c is unclear, as there are few documented cases. Elmhamdi et al. (2004) attributed the blueshifted lines in the SN Ib 1990I to condensation of dust in the ejecta around day 250 after explosion. In most cases, however, the asymmetric line profiles in SNe Ib/c have different interpretations. Sollerman et al. (1998), for example, argue that the blueshifted lines in the ejecta of the SN Ib 1996N were due to intrinsic asymmetry in the ejecta and not the effect of dust obscuration described above. The blueshifted profiles in SN 1993J, which transitioned from Type II to Type Ib, have been interpreted as a result of either clumping or optically thick ejecta (Wang & Hu 1994; Filippenko et al. 1994), but not dust formation.

By contrast, we find very clear evidence in the spectra of SN 2006jc that grain formation is affecting the line profiles as described above, although the way it manifests itself is unusual compared to all other SNe with this type of evidence for dust. Specifically, the net blueshift and asymmetry are seen primarily in the strong intermediate-width He I emission lines that arise in the CSM or post-shock shell (see §6.1), while the effect is not seen in broad lines from the SN ejecta.

Figure 4 shows the line profiles of the two strongest intermediate-width He I lines in the optical spectrum of SN 2006jc as a function of time, while Figure 5 shows He I $\lambda 7065$ alone, with all epochs aligned and plotted over one another for direct comparison of the line-profile evolution. These lines, He I $\lambda 5876$ and $\lambda 7065$, are relatively free from P-Cygni absorption, which complicates the interpretation of He I lines superposed on the strong blue continuum (Paper I). Figures 4 and 5 display a clear systematic evolution of the He I line profile with time.

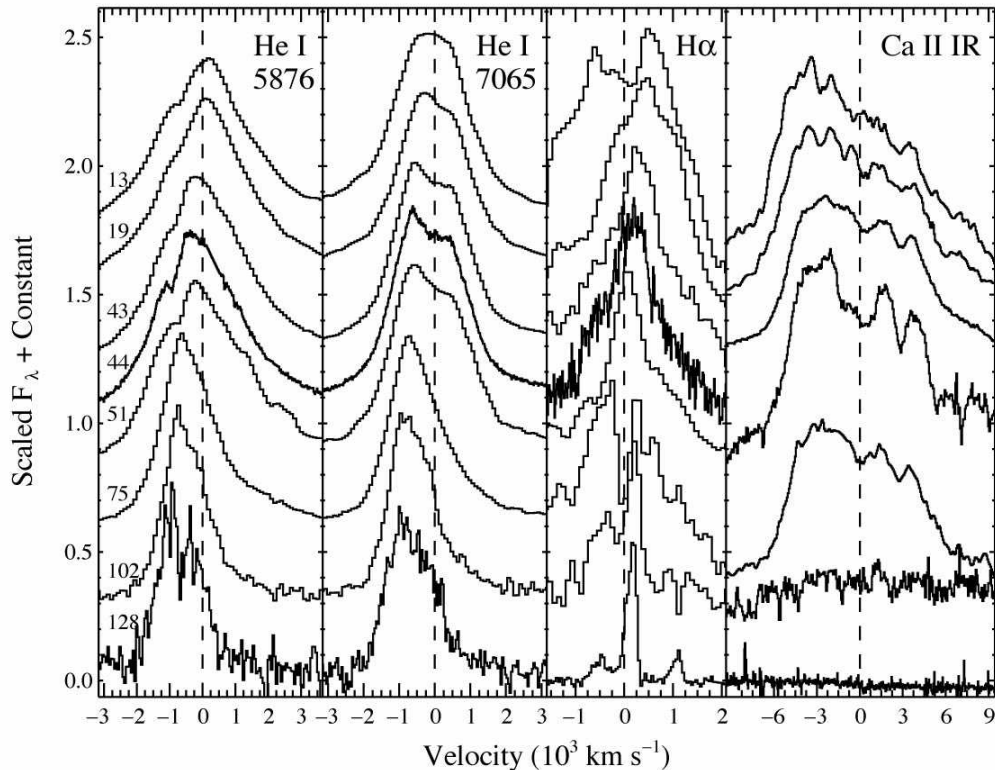


FIG. 4.— Temporal evolution of the intermediate-width He I $\lambda 5876$ and $\lambda 7065$ emission-line profiles in SN 2006jc from early times (day 13) through our last spectrum in the nebular phase at day 128. The He I lines show clear changes in their line profiles, becoming progressively more asymmetric and blueshifted, presumably due to increased obscuration from freshly synthesized dust. $H\alpha$ and the broad Ca II near-IR triplet, on the other hand, do not exhibit this effect. $H\alpha$ shows irregular profile changes, but they are not systematically shifted to the blue, while Ca II simply fades entirely during the putative time of dust formation. This gives an important clue to the location of the new dust (see text §5). (Note that in the last two spectra, the very narrow component of $H\alpha$ is probably from a superposed H II region. Also, the Ca II profile is missing for day 44 because the spectrum on that date did not reach sufficiently long wavelengths.)

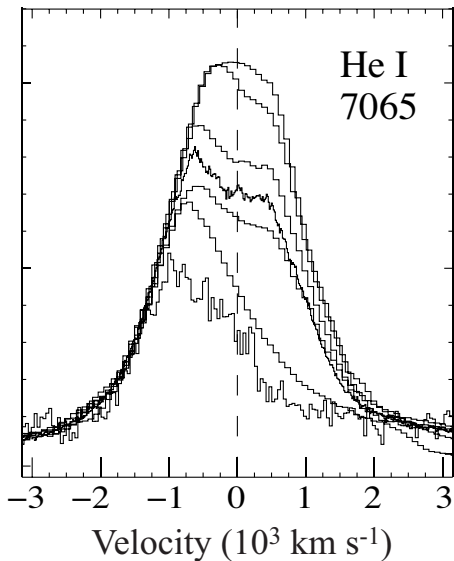


FIG. 5.— Same as in Figure 4, but showing only He I $\lambda 7065$ with all epochs scaled and superposed on one another to emphasize the change in line profile.

Since the lines appear nearly symmetric at early times, this effect is not attributable simply to intrinsic asymmetries in the ejecta. It also cannot be due to optically thick ejecta as is thought to be the case for SN 1993J (Wang & Hu 1994; Filippenko et al. 1994), since that interpretation would predict the lines to start very asymmetric

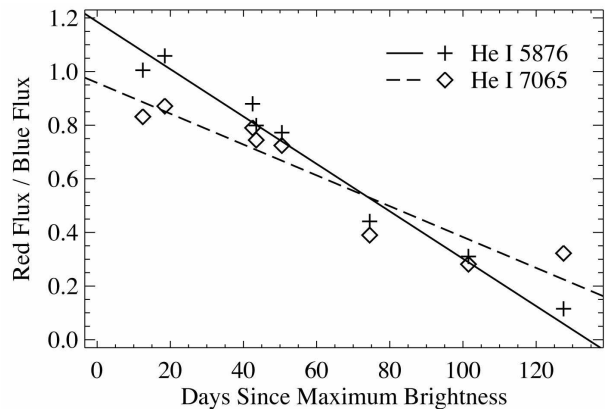


FIG. 6.— The data in this plot document the fading of the red half of the intermediate-width He I lines with time, as compared to the blue side of the lines. The plotted quantity is the ratio of the line flux at positive velocities to the flux at negative velocities, relative to the assumed systemic velocity shown with a dashed line in Fig. 4 and 5. The straight lines show least-squares fits to the declining red/blue ratio of each line, with slopes of -0.88 ± 0.08 per 100 d for $\lambda 5876$ and -0.58 ± 0.09 per 100 d for $\lambda 7065$. The last datum for $\lambda 5876$ was not included in the fit because of contamination from Galactic Na I D absorption, but this had little effect on the slope. The fact that these slopes are significantly different is probably the effect of reddening from small grains, causing more severe extinction in $\lambda 5876$ than in $\lambda 7065$.

and to become progressively *less* asymmetric with time — exactly the opposite of what we observe in SN 2006jc. Instead, the increasing asymmetry with time implicates

dust formation in SN 2006jc. The He I profiles begin to show subtle effects of asymmetry around days 40–50, but they become more severely asymmetric by day 75. Notably, this epoch between day 51 and day 75 that shows the strongest decrease in the red side of the lines is also the same time during which the red/IR continuum appeared and when the blue continuum faded.

This severe asymmetry seen by day 75 persists through days 102 and 128. By day 128 the red/IR continuum emission component had disappeared (Fig. 2), while the obscuration of the red side of the He I lines remained. The newly formed dust was not destroyed; its red emission simply faded because the dust cooled so that its bolometric flux shifted to longer wavelengths, while its influence through extinction persisted.

Figure 6 quantifies the time-dependent asymmetry of the He I lines, where we show the integrated flux ratio of the red side of the line to the blue side. He I $\lambda 5876$ and $\lambda 7065$ exhibit slightly different behavior in the way their red flux decreases with time. Least-squares fits to the data indicate that the asymmetric obscuration effect is more pronounced in He I $\lambda 5876$ than in $\lambda 7065$, with statistically significant differences in the slopes of their respective declining red/blue ratios (Fig. 6). Since $\lambda 5876$ has a shorter wavelength than the other, we might expect it to be more severely affected by dust obscuration if the grains are small compared to the observed wavelength. This supports our assumptions about the grain size made in §3 and Figure 3. Of course, the trends in Figure 6 may not follow straight lines. In fact, the sharpest decrease appears between days 50 and 75, as noted earlier, which is when the red/IR emission strengthened. The red side of the line decreases to roughly 40% of the emission on the blue side, indicating a visual-wavelength extinction of roughly 1 mag toward the far side of the SN.

5. RULING OUT LIGHT-ECHO MODELS

The leading explanation for IR excess emission in SNe IIn is a light-echo model, where radiation from the SN propagates outward into the pre-SN circumstellar ejecta. In doing so it illuminates and heats pre-existing dust formed in the progenitor’s wind (Gerardy et al. 2002; Fassia et al. 2000; Emmering & Chevalier 1988; Dwek 1983; Bode & Evans 1980).

SN 2006jc is unique in that it was observed to have an LBV-like eruption 2 yr before the SN, creating a dense environment. Normal LBV eruptions are known to be copious dust producers (e.g., Smith et al. 2003), so we cannot exclude the possibility of considerable dust in the CSM around SN 2006jc. Thus, we consider whether an IR echo can explain our observations of SN 2006jc, but we find that it cannot for two main reasons.

First, the dust around SN 2006jc was much hotter (~ 1600 K) than that in SNe II (a few hundred K). It stayed at a roughly constant temperature until it disappeared quickly, whereas IR light echoes tend to decay slowly on timescales of years (Gerardy et al. 2002). These hints point toward newly formed dust rather than dust at large radii that is radiatively heated by a central engine.

Second, the evolution of the He I line profiles indicates an amount of obscuring dust that increases systematically with time. In an IR-echo model, the amount of dust and the extinction it causes stay constant with time or may even decrease. Furthermore, such dust would be

at large radii and would not selectively absorb red sides of the line profiles. Thus, we can rule out an IR echo as the principal agent for the dust seen in SN 2006jc.

6. WHERE IS THE NEW DUST LOCATED?

Sometime between days 51 and 75, several events occurred simultaneously in the spectroscopic evolution of SN 2006jc which are relevant to the interpretation of dust formation in this object.

(a) SN 2006jc developed a strong red/IR continuum excess emission component, which can be accounted for by hot graphite grains at around 1600 K, or silicates at slightly higher temperatures. In both cases, the grains are likely to be smaller than the observed wavelength.

(b) The intermediate-width He I line profiles became severely asymmetric and blueshifted, suggesting that the redshifted emitting material has been largely obscured. This effect was more pronounced at shorter wavelengths, again pointing to relatively small grain radii.

(c) The strong blue continuum faded relative to the red continuum for the first time, and the broad emission lines tracing the SN ejecta (like Ca II and O I) faded. Unlike the He I lines, the broad SN ejecta emission lines did not show obvious blueshifts or more asymmetric profiles — they simply faded (Fig. 4). At the same time, the *B*-band light curve started to fade faster than the ^{56}Co decay rate (Paper I).

The details of how these changes happened help to unravel the geometry of the SN ejecta. In particular, they provide clues to the relative locations of the obscuring and emitting dust, the intermediate-width He I lines, the blue continuum, and the broad emission lines.

Figure 7 shows a cartoon of the possible geometry of SN 2006jc, limited to the structures relevant for interpreting effects of dust. We assume spherical symmetry for simplicity, but the discussion below does not preclude possible asymmetry in the SN ejecta or the bipolar geometry that is likely in circumstellar matter arising from LBV-style eruptions (e.g., Smith 2006; Owocki 2003). We can estimate the outer radius of the dense He shell ejected in the 2004 event as $v_W \times \Delta t \approx 2000 \text{ km s}^{-1} \times 2 \text{ yr} \approx 1000 \text{ AU}$. The radius of the blast wave is $v_{\text{shock}} \times \Delta t$, so for a shock speed of $\sim 10^4 \text{ km s}^{-1}$, the timescale for the shock to sweep through most of the He shell is $\sim 100\text{--}200 \text{ d}$. This is comparable to the timescale of our observations, so we might expect significant changes as swept-up material accumulates.

6.1. The Emitting He I Region

Before determining the zone in Figure 7 where the dust formation occurs, we must first understand the origin of the bright intermediate-width He I lines, potentially coming from the pre-shock WR wind or the post-shock shell. Both the wind or post-shock origin are plausible, in principle, since the progenitor star was thought to be a WR star, and such stars have fast winds capable of producing the observed He I linewidths. Figure 8a shows the time evolution of line fluxes for He I lines in SN 2006jc measured from our spectra.

In general, the emission-line fluxes decline with time at a rate commensurate with the drop in the red continuum level. The red continuum in Figure 8a represents the assumed continuum at the time of each line measurement,

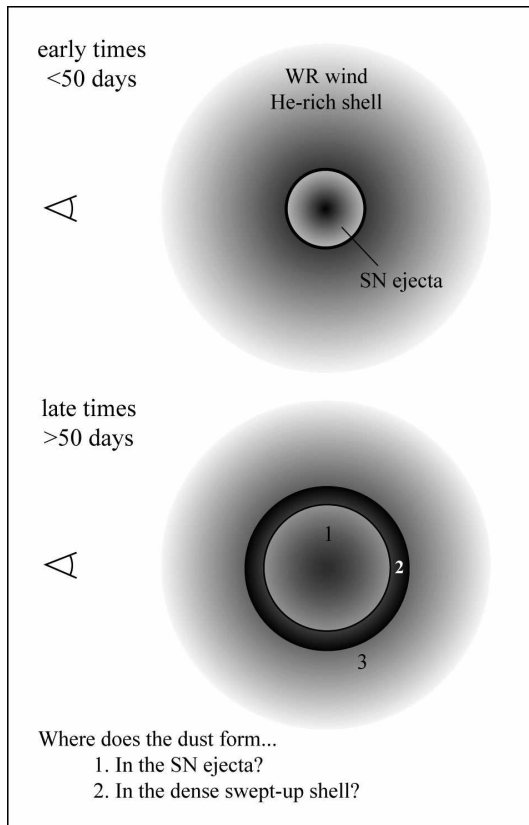


FIG. 7.— Sketch of a simplified SN 2006jc geometry for the purpose of discussing where the dust forms. The top sketch is at early times, when the SN blast wave has started plowing into the He-rich CSM, but has not yet swept up much mass. The bottom sketch is at later times, closer to the epoch of dust formation, when a thicker, dense shell has developed in the cooling zone behind the forward shock. The two locations where dust is likely to form are zone 1 in the SN ejecta themselves as they cool enough to allow condensation (this is the same zone that gives rise to the broad Ca II and O I emission), or zone 2 in the dense shell of swept-up gas between the reverse shock and the forward shock. There are geometrical reasons to favor zone 2 as the most likely region of dust formation. Intermediate-width He I lines arise in zone 2 and/or 3, close to the blast wave where the densities are high.

interpolated from the R -band light curve in Paper I. As noted earlier, we extrapolated the decline rate to infer the red continuum flux at the latest epochs. Since we calculated line fluxes using these continuum values, uncertainties in line fluxes are large at late times (we adopt generous 10–20% error bars in Fig. 8). However, since fluxes for various lines measured in the same spectrum at each epoch are scaled using the same continuum, the uncertainty in *relative* line fluxes is much smaller.

Of particular interest is He I $\lambda 7065$, which seems to counter the trend exhibited by the other two He I lines in Figure 8a. Namely, it has a slower decline rate, becoming more prominent in the spectrum with time.

More telling is Figure 8b, which shows the time evolution of the He I $\lambda 7065/\lambda 5876$ flux ratio. These are the two brightest lines in the spectrum, so measurement uncertainties are small. We see that He I $\lambda 7065$ is only half as strong as $\lambda 5876$ at early times, and continually grows until the lines have equal flux at late times. This effect is not due simply to wavelength-dependent extinction by dust, since it is not seen in the He I $\lambda 6678/\lambda 5876$ flux ratio, also shown in Figure 8b.

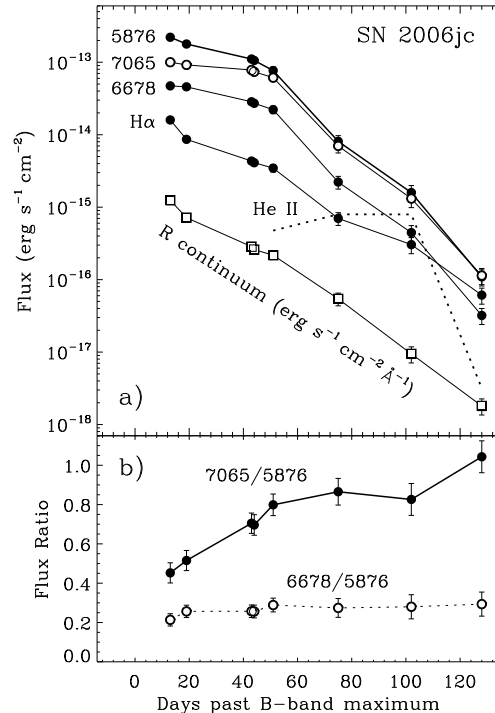


FIG. 8.— Time evolution of emission-line fluxes in SN 2006jc. Panel (a) shows the measured flux for bright He I lines and H α , compared to the decline rate of the red (~ 6500 Å) continuum (in F_λ units) on the same dates as the emission-line measurements, interpolated and extrapolated from R -band photometry from Paper I as described in the text. The dashed curve shows the measured line flux of He II $\lambda 4686$ on days 75 and 102, where the first and last values on days 51 and 128, respectively, are upper limits (the uncertainty in the He II fluxes on days 75 and 102 are about 10%). Panel (b) shows the observed ratios of He I $\lambda 7065$ (solid line, filled circles) and $\lambda 6678$ (dashed, unfilled) to $\lambda 5876$ on the same dates.

If the He I lines arise primarily in the CSM, then their flux should drop with time as observed because they result from photoexcitation by the SN light. However, in this scenario it is difficult to understand the growing He I $\lambda 7065/\lambda 5876$ ratio, which is a hallmark of increasing density, because the density of the CSM should drop as r^{-2} .

On the other hand, if the He I lines arise primarily in the post-shock gas it could explain the high densities inferred from the $\lambda 7065/\lambda 5876$ ratio, but we might expect their flux to be constant with time or even to increase as more material enters the post-shock shell.

To explain the evolution of relative He I line strengths, then, we propose a hybrid scenario, where the observed He I lines are emitted from *both* the unshocked CSM and the post-shock shell — but where their relative contributions to the spectrum change with time. At early times (upper sketch in Fig. 7), the emission from the unshocked CSM has the advantage of a large emitting volume, so it dominates the spectrum. At late times, the post-shock emission takes over for two basic reasons. First, the shock has swept through much of the CSM volume and placed more of the He gas in the post-shock region, detracting from the CSM emission that is dropping anyway because of the decline in UV radiation. Second, the much higher density of post-shock gas ($n_e \approx 10^{10}$ cm $^{-3}$ for $F(\lambda 7065)/F(\lambda 5876) \gtrsim 1$; see §6.3) has the advantage that emission is proportional to n_e^2 , making it increasingly dominant with time as more material passes

through the shock. In this model, we might expect the He I line widths to increase with time, but if this effect is present, it is hidden by growing extinction from dust, making the lines asymmetric (Fig. 5).

Lastly, we note that Figure 8a also shows the evolution of the H α line flux with time, indicating that it too grows stronger compared to He I λ 5876. However, this increase in the relative strength of H α is most likely due simply to increased contamination from a background H II region. Since the H II region will be constant with time, it will contribute relatively more to the spectrum as the SN light fades. At late times, the H α line is dominated by a very narrow (unresolved) line with neighboring [N II] lines typical of H II regions. The intermediate-width component of H α is barely visible at late times, contributing less than 5% of the total flux. By contrast, such narrow (unresolved) components for He I are not seen.

6.2. Zones 1, 2, and 3

At early times shown in the top panel of Figure 7, the SN ejecta occupy a small volume compared to the He-rich WR wind, and the blast wave has swept up relatively little mass. The top panel corresponds to the early epochs of spectra discussed in Paper I. The late-time spectra discussed here correspond to the lower panel in Figure 7, when the central SN ejecta (zone 1) have faded and when a significant fraction of the mass in the CSM (zone 3) has been swept up to form part of a dense shell between the forward and reverse shocks (zone 2). The broad emission lines like the Ca II near-IR triplet and O I λ 7774 originate in zone 1, while the intermediate-width He I lines originate in zone 3, the outer part of zone 2, or both. Again, if the progenitor was a WR star, its likely wind speeds of 1000–2000 km s⁻¹ are sufficient to explain the intermediate-width lines. The strong blue/UV continuum also originates in zone 1, because blue He I lines show P Cygni absorption of the blue continuum, whereas red He I lines do not (Paper I). Since there are singlet and triplet He I lines in both wavelength ranges, the likely reason for the presence of P Cygni absorption in the blue and not in the red is probably related to the geometry or the strength of the blue continuum.

Given the hypothetical geometry in Figure 7, consider the observational consequences for the two likely locations where the dust in question may have formed, which are in the SN ejecta (zone 1) or in the dense swept-up shell (zone 2):

(1) If dust grains form in the SN ejecta in zone 1, they can only block part of the total He I emission from the observer, and would therefore only influence the directly receding material in the red wings of the He I lines. Dust grains in this central region would not be able to absorb any of the He I emission near the systemic velocity, and therefore cannot account for the observed He I line profiles from day 75 onward, when most of the red emission and some of the zero-velocity emission is absorbed. Additionally, dust forming within the SN ejecta would be expected to preferentially absorb emission from redshifted SN ejecta, leading to asymmetric Ca II and O I line profiles. These are not observed (Fig. 4), so we conclude that it is unlikely that the dust has formed in the SN ejecta in zone 1.

(2) If instead the dust grains form in the dense swept-up shell in zone 2, then they can efficiently prevent much

of the He I emission from reaching the observer, because He I lines are formed in a region with a similar extent. This could explain the line profiles in Figures 4 and 5. Also, dust formed in zone 2 would absorb emission from the SN ejecta equally at all velocities, consistent with the lack of blueshifted profiles in the broad Ca II and O I lines. Since the blue continuum probably arises in zone 1, dust formed in zone 2 could also explain its fading by day 75 (Fig. 1). For these reasons, we consider it more likely that grains are condensing in the swept-up shell in zone 2.

6.3. Steady-State Dust Formation in the Post-Shock Gas

At first glance, it seems somewhat odd that the apparent grain temperature around 1600 K stayed nearly constant (Fig. 2) for about a month after Christmas 2006, and then after another month (by mid-February 2007) the dust had cooled rapidly enough to be invisible at optical wavelengths. This would be difficult to understand in a scenario where the grains condense directly in the SN ejecta (zone 1 in Fig. 7) and are warmed by a declining luminosity from radioactive decay; in fact, this interpretation seems impossible because the SN ejecta have insufficient luminosity to heat the dust (see §3.2). However, if the grains are forming in the dense swept-up shell (zone 2 in Fig. 7) as we suspect, there may be a reasonable explanation as follows.

When a blast wave encounters and sweeps through a dense circumstellar shell, we can hypothesize that grains may continuously form at $T \approx 1600$ K as dense material rapidly cools behind the shock front. This may continue as long as sufficiently dense matter enters the shock. How dense is the post-shock gas? As noted earlier, we measure an unusually high flux ratio of He I λ 7065/ λ 5876, approaching unity (Fig. 8b). This was seen in SN 1999cq as well (Matheson et al. 2000). Following Almgren & Netzer (1989), this would seem to indicate electron densities of almost 10^{10} cm⁻³ (although their calculations were for He embedded in H-rich gas), or mass densities of $\sim 3 \times 10^{-14}$ g cm⁻³ for ionized He gas. Coincidentally, this value is compatible with the expected critical density for graphite dust precipitation (e.g., Clayton 1979). Such high densities are far too high to exist in the CSM, because they would require mass-loss rates greater than $10 M_{\odot}$ yr⁻¹ at $R = 500$ AU for a wind speed of ~ 2000 km s⁻¹, and would obscure our sightline to the SN.

Instead, these densities are only likely to be found in the post-shock cooling zone where material piles up. Coincidentally, efficient He II λ 4686 emission, which is correlated with the dust emission as discussed next in §7, also requires densities of order 10^{10} cm⁻³ (e.g., Martin et al. 2006). From our observations alone we cannot differentiate between dust forming in CSM gas swept up by the forward shock, or instead, C-rich SN ejecta that have passed the reverse shock. However, the overlap with the conditions leading to dust formation in the C-rich colliding winds of WC+O binaries described in §7 would add weight to the latter option in the case of SN 2006jc. Detailed models of dust formation in dense shocks would be interesting to pursue in this regard.

The hot dust that forms will cool rapidly and its optical emission will fade, but it will continuously be re-

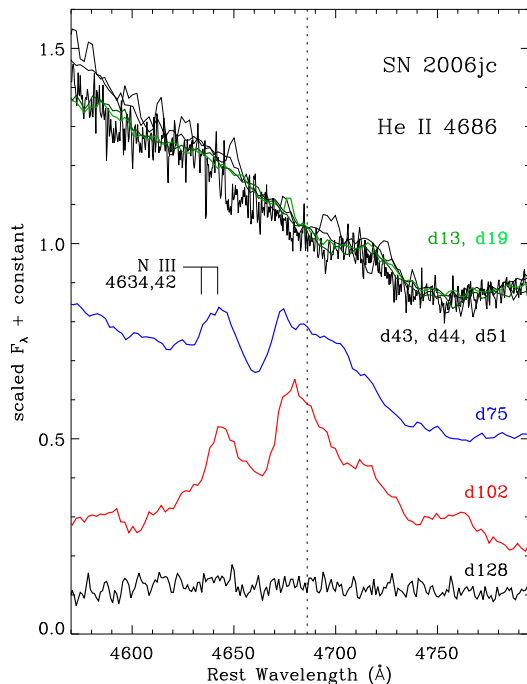


FIG. 9.— Similar to Fig. 1, but emphasizing the wavelength range around He II $\lambda 4686$. The early-time spectra of days 13 through 51 show no evidence for an emission feature that can be associated with He II. A prominent, intermediate-width (FWHM ≈ 2000 km s $^{-1}$) emission feature that could be He II $\lambda 4686$ (dashed vertical line) with an irregular line profile is seen at day 75, strengthens by day 102, and then disappears completely by day 128. Thus, the He II emission feature follows the same temporal behavior as the red continuum from dust in Figure 1. The relatively narrow emission feature on the blue side of the line is probably N III $\lambda 4640$.

plenished as long as the shock is sweeping up sufficiently dense matter. Thus, the freshly synthesized dust at the hottest temperatures will always dominate the flux at the shortest wavelengths that we observe here. This steady-state phase may continue until the shock passes beyond the densest part of the LBV-like shell, when the density drops below the critical threshold for grain nucleation. Optical spectra of SN 2006jc in Figure 2 suggest that this phase lasted about $\Delta t \gtrsim 1$ month, implying a thickness for the hypothetical shell of roughly 50–200 AU for blast wave expansion speeds of 2,000–10,000 km s $^{-1}$. Perhaps it is only a coincidence that the radial thickness of the massive dust shell around η Carinae is a few hundred AU as well (Smith 2006). In any case, the 1-month-long constant-temperature phase seen in the red continuum feature (Fig. 2) suggests that its *emitting* dust is consistent with a scenario involving dust formation in a dense swept-up shell, like the *obscuring* dust discussed above.

7. He II $\lambda 4686$, DUST FORMATION, AND ETA CARINAE

The CSM that is struck and swept up by the forward shock will be a hot, X-ray-emitting plasma that must cool efficiently in order to form dust grains. Understanding this process will require detailed calculations of the shock interaction that are well beyond the scope of our paper. Nevertheless, we argue that this scenario is plausible because it has a related observational precedent: dust formation is known to occur in the strong colliding-wind shocks of WC+O binaries (e.g., Allen et al. 1972; Gehrz & Hackwell 1974; see also Crowther 2003 for a

review). How dust is able to form in these inhospitable conditions is not fully understood either, but clearly nature is able to overcome this obstacle in the compressed post-shock gas because the evidence for dust formation in these systems is unambiguous.

Prototypes of the dust-forming late-type WC binaries are the persistent dust producers like WR104 and WR98a (the so-called “pinwheel” systems; Tuthill et al. 1999; Monnier et al. 1999) and the episodic dust producers in eccentric binaries like WR140 (Monnier et al. 2002). In such systems, strong colliding-wind shocks compress and heat He-rich and C-rich gas to temperatures capable of emitting strong X-rays (e.g., Usov 1999). As the gas proceeds down the shock cone, it then cools rapidly enough to produce graphite dust before dispersing. These conditions closely mirror the shocked shell (zone 2 in Fig. 7) of SN 2006jc, which is also an X-ray source (Immler et al. 2008). Thus, in the case of SN 2006jc, the C-rich SN ejecta passing through the reverse shock might provide the necessary seeds for grain nucleation. As noted earlier, another clue that the dust may be C-rich is that it appears to condense at a temperature of ~ 1600 K, higher than the temperatures at which silicate grains are normally seen to condense.

Another eccentric colliding-wind binary that looks almost identical to WR140 in X-rays is η Carinae (see, e.g., Corcoran 2005 for a review and references), where X-ray emission is thought to result from the collision of a dense and relatively slow LBV wind with a faster $\sim 3,000$ km s $^{-1}$ O-star wind (thus, the characteristic shock velocities may be similar to those of SN 2006jc). In η Carinae, X-ray emission is relatively weak for most of the ~ 5 yr orbit, but the strength of X-rays greatly intensifies as the system approaches periastron when the post-shock density increases dramatically. At the same time, strong near-IR excess emission develops and continues to rise toward periastron along with the X-ray emission (e.g., Whitelock et al. 2004). The coincidence of X-ray emission and near-IR excess emission is reminiscent of SN 2006jc, although in η Car it is not known if the near-IR excess is due to newly formed hot dust grains in shocks. In η Carinae, the rise of X-rays and near-IR emission around periastron is also accompanied by a brief occurrence of He II $\lambda 4686$ emission that is weak or absent from the spectrum at all other times (Steiner & Damiani 2004; Martin et al. 2006). This may hint at a link of common physical conditions that are required to produce X-rays, a near-IR excess, and He II emission in dense shocks.

In that case, the spectra of SN 2006jc in Figure 8 become quite intriguing. An emission feature that can plausibly be identified as He II $\lambda 4686$ is seen in the spectrum. It is an intermediate-width feature much like the He I lines, spanning roughly ± 2500 km s $^{-1}$. It has an irregular double-peaked shape because it is accompanied by N III $\lambda\lambda 4634,4642$ emission in its blue wing that directly varies with the strength of He II $\lambda 4686$. Following comments in § 1, it is curious that these features are also defining characteristics of the dense winds in Of/WN stars.

Figure 8a shows the He II $\lambda 4686$ flux as a function of time with a dotted line, where the first and last points are upper limits because the line was only detected on days 75 and 102. Days 75 and 102 showed nearly identical He II $\lambda 4686$ line fluxes of $\sim 10^{-15}$ erg s $^{-1}$ cm $^{-2}$ (excluding

N III), translating to an intrinsic luminosity of $1.3 \times 10^4 L_{\odot}$ if we adopt a distance modulus $m - M = 31.8$ mag as before. The 4686 Å line probably represents about 1% of the cooling by all He II recombination lines. If so, then He II recombination contributes $\sim 10\%$ of the UV/visual luminosity of the SN. Thus, either photoexcitation or shock energy could power the He II lines.

The important point, though, is that the feature around 4686 Å is seen *only* in the day 75 and day 102 spectra — precisely the same epochs when the strong red/IR continuum emission from dust is present (Fig. 1–3). It is completely absent in the early-time spectra, and it disappears by the time of our last spectrum on day 128, just like the hot-dust emission. This coincidence can be taken as further supporting evidence that the dust formation in SN 2006jc occurs in the post-shock gas (zone 2), where the He I and He II emission arise, analogous to the dust formation in colliding-wind binaries.

Since He II $\lambda 4686$ and the IR excess emission from dust seem to track one another in SN 2006jc and are apparently associated with a strong shock event, it seems reasonable to predict that the X-rays from SN 2006jc may behave similarly with time. In fact, Immler et al. (2008) recently noted a distinct and very unusual increase in the X-ray flux of SN 2006jc that lasted for a few months and coincided precisely in time with our proposed epoch of dust formation and enhanced He II $\lambda 4686$ emission in Figure 8a. This coincidence suggests a common link.

What does this imply for η Carinae, which shows nearly identical behavior of X-rays, He II $\lambda 4686$ emission, and near-IR excess emission appearing for only a short time? In SN 2006jc, the case for newly formed dust grains in the post-shock gas seems solid. We conjecture, then, that the near-IR excess in η Carinae is also the result of emission from hot (~ 1600 K) dust grains that have formed in the dense post-shock gas in the colliding wind interaction region where gas can evidently cool rapidly enough. After this paper was submitted for publication, we learned that Kashi & Soker (2007) independently came to a similar conclusion.

8. SUMMARY

Based on the red/near-IR continuum excess emission that can be explained by hot dust at 1600–1700 K, as well as the systematically more asymmetric and blueshifted He I emission lines, we propose that SN 2006jc began to form significant amounts of hot dust between 50 and 75 d after peak luminosity. This dust-formation epoch continued for at least a month or more, and then apparently ceased. Based on this behavior, a number of geometric considerations, and the transient He II $\lambda 4686$ emission, we argue that the dust formed in a dense shell of shocked gas and not in the SN ejecta. Grain formation in this post-shock shell may also help account for why the dust formed so soon after explosion — sooner than in any other dust-forming SN. The shell could have been composed of dense CSM ejected by an LBV-like event observed 2 yr prior to the SN (Paper I; Pastorello et al. 2007), which was then swept up by the forward shock. Alternatively, grains may have condensed from C-rich SN ejecta that passed the reverse shock when the blast wave decelerated upon impact with the LBV-like shell. Either hypothesis would be consistent with our observational constraints that place the dust somewhere

between the forward and reverse shocks (zone 2 in Fig. 7). The dust-formation epoch lasted for a brief phase when the swept-up material behind the shock was sufficiently dense and cooling quickly enough for refractory elements to condense.

Few other SNe Ib/c have shown any evidence for dust, and SN 2006jc may now provide the least ambiguous case where new dust has formed. We suspect that this — like most of the other unusual properties of SN 2006jc — is a direct consequence of the dense circumstellar environment around SN 2006jc ejected during the LBV-like eruption just before explosion. One obvious speculation is that SN 1999cq and SN 2002ao, which had similar spectra to SN 2006jc (see Paper I), may also have undergone episodic mass ejection shortly before they exploded. SN 2006jc, SN 2002ao, and especially SN 1999cq had very rapidly declining optical light curves compared to most other SNe Ib/c (Paper I). Although the dust effects discussed in this paper were not documented for either SN 2002ao or SN 1999cq, their rapid declines may have been accompanied by dust formation. It will be interesting to see if such a connection between LBV-like precursor events and SNe Ib/c with intermediate-width lines can be established with a future example.

Given the rarity of dust formation in SNe Ib/c and the scarcity of dense circumstellar environments like those of SNe 2006jc, 1999cq, and 2002ao, one might conclude that most SNe Ib/c are *not* preceded by an LBV-like eruption, and that SN 2006jc is therefore a special case.

The presence of weak hydrogen emission in the spectrum, and the occurrence of an LBV-like outburst just before the SN, would seem to imply that SN 2006jc was a young WN star that was still in the last phases of transitioning from the LBV phase (Paper I). This seems at odds, though, with the fact that SN 2006jc was basically a Type Ic event with an external He-rich CSM, implying that it also recently removed its He layer in an abrupt transition to the WC phase. (No WC stars are known to contain H, while some WN stars do; see Smith & Conti 2008.) Even if the ejected layer had retained some H because of previous mixing, that mixing must not have reached into deeper layers. Alternatively, Pastorello et al. (2007) proposed that the mystery of the CSM of SN 2006jc might be explained by invoking a less-evolved companion star in the system that had a classical LBV eruption. However, transferring the mysterious LBV event to a hypothetical companion still does not account for why the CSM was H poor. In any case, this overlap is reminiscent of SNe that blur the distinction between Types Ib and II, like SN 1987K (Filippenko 1988) and SN 1993J (e.g., Filippenko et al. 1993), and is mirrored by the ambiguity between LBVs and H-rich WN stars noted in § 1.

Altogether, then, these clues suggest that rapid evolution through episodic LBV-type mass-loss events may play a significant role in both the onset and the progression of the WR phase. Just as giant LBV eruptions may drive the evolution from H-rich to H-poor stars (Smith & Owocki 2006), perhaps similar events in WR stars can, in rare cases, drive the evolution from WN to WC as suggested by SN 2006jc. In this context, it is worth emphasizing that if the progenitor of SN 2006jc had undergone core collapse only 5–10 yr ago, it would have probably appeared as a relatively normal Type Ib event.

We gratefully acknowledge discussions with R. Chornock, M. Ganeshalingam, W. Li, M. Modjaz, K. Nomoto, T. Nozawa, and C. Fransson. Most of the data presented herein were obtained at the W. M. Keck Observatory, which is operated as a scientific partnership among the California Institute of Technology, the University of California, and the National Aeronautics and Space Administra-

tion. The Observatory was made possible by the generous financial support of the W. M. Keck Foundation. We thank the Keck and Lick Observatory staffs for their assistance. This research was supported by NSF grant AST-0607485. Support for this work was also provided by NASA through awards (Programs 20256 and 30292) issued by JPL/Caltech.

REFERENCES

- Allen, D. A., Harvey, P. M., & Swings, J. P. 1972, *A&A*, 20, 333
 Almog, Y., & Netzer, H. 1989, *MNRAS*, 238, 57
 Arkharov, A., Efimova, N., Leoni, R., Di Paola, A., Di Carlo, E., & Dolci, M. 2006, *ATel*, 961, 1
 Barbá, R. H., Niemela, V. S., Baume, G., & Vazquez, R. A. 1995, *ApJ*, 446, L23
 Bode, M. F., & Evans, A. 1980, *MNRAS*, 193, 21
 Bohannan, B., & Walborn, N. R. 1989, *PASP*, 101, 520
 Burke, J. R., & Hollenbach, D. J. 1983, *ApJ*, 265, 223
 Cernuschi, F., Marsicano, F., & Codina, S. 1967, *Annales D'Astrophysique*, 30, 1039
 Clayton, D. D. 1979, *ApSS*, 65, 179
 Colgan, S. W. J., Haas, M. R., Erickson, E. F., Lord, S. D., & Hollenbach, D. J. 1994, *ApJ*, 427, 874
 Corcoran, M. F. 2005, *AJ*, 129, 2018
 Crowther, P. A. 2003, *Ap&SS*, 285, 677
 Crowther, P. A. 2007, *ARAA*, in press
 Crowther, P. A., Hillier, D. J., & Smith, L. J. 1995, *A&A*, 293, 172
 Danziger, I. J., Gouiffes, C., Bouchet, P., & Lucy, L. B. 1989, *IAU Circ.*, 4796, 1
 Draine, B. T., & Lee, H. M. 1984, *ApJ*, 285, 89
 Dwek, E. 1983, *ApJ*, 274, 175
 Dwek, E., et al. 1983, *ApJ*, 274, 168
 Dwek, E., Moseley, S. H., Glaccum, W., Graham, J. R., Loewenstein, R. F., Silverberg, R. F., & Smith, R. K. 1992, *ApJ*, 389, L21
 Elmhamdi, A., Danziger, I. J., Chugai, N., Pastorello, A., Turatto, M., Cappellaro, E., Altavilla, G., Benetti, S., Patat, F., & Salvo, M. 2003, *MNRAS*, 338, 939
 Elmhamdi, A., Danziger, I. J., Cappellaro, E., Della Valle, M., Gouiffes, C., Phillips, M. M., & Turatto, M. 2004, *A&A*, 426, 963
 Emmering, R. T., & Chevalier, R. A. 1988, *AJ*, 95, 152
 Faber, S. M., et al. 2003, *Proc. SPIE*, 4841, 1657
 Fassia, A., et al. 2000, *MNRAS*, 318, 1093
 Filippenko, A. V. 1988, *AJ*, 96, 1941
 Filippenko, A. V. 1997, *ARAA*, 35, 309
 Filippenko, A. V., Matheson, T., & Barth, A. J. 1994, *AJ*, 108, 2220
 Filippenko, A. V., Matheson, T., & Ho, L. C. 1993, *ApJ*, 415, L103
 Filippenko, A. V., Barth, A. J., Bower, G. C., Ho, L. C., Stringfellow, G. S., Goodrich, R. W., & Porter, A. C. 1995, *AJ*, 110, 2261 [Erratum: 1996, *AJ*, 112, 806]
 Foley, R. J., Smith, N., Ganeshalingam, M., Li, W., Chornock, R., & Filippenko, A. V. 2007, *ApJ*, 657, L105 (Paper I)
 Gal-Yam, A., et al. 2007, *ApJ*, 656, 372
 Gehrz, R. D. 1988, *ARA&A*, 26, 277
 Gehrz, R. D. 1999, *Phys. Rep.*, 311, 405
 Gehrz, R. D., & Hackwell, J. A. 1974, *ApJ*, 194, 619
 Gehrz, R. D., & Ney, E. P. 1989, *Proc. Nat. Acad. Sci.*, 87, 4354
 Gerardy, C. L., et al. 2002, *ApJ*, 575, 1007
 Gilman, R. C. 1974, *ApJS*, 28, 397
 Goodrich, R. W., Stringfellow, G. S., Penrod, G. D., & Filippenko, A. V. 1989, *ApJ*, 342, 908
 Hoyle, F., & Wickramasinghe, N. C. 1970, *Nature*, 226, 62
 Immler, S., et al. 2008, *ApJ*, in press (astro-ph/0712.3290)
 Kashi, A., & Soker, N. 2007, preprint
 Koenigsberger, G. 2004, *Rev. Mex. AA*, 40, 107
 Koenigsberger, G., et al. 2000, *ApJ*, 542, 428
 Kotak, R., & Vink, J. S. 2006, *A&A*, 460, L5
 Leonard, D. C., Filippenko, A. V., Barth, A. J., & Matheson, T. 2000, *ApJ*, 536, 239
 Lucy, L. B., Danziger, I. J., Gouiffes, G., & Bouchet, P. 1989, in *Structure and Dynamics of the Interstellar Medium*, ed. G. Tenorio-Tagle, et al. (Berlin: Springer-Verlag), 164
 Martin, J. C., Davidson, K., Humphreys, R. M., Hillier, D. J., & Ishibashi, K. 2006, *ApJ*, 640, 474
 Matheson, T., Filippenko, A. V., Chornock, R., Leonard, D. C., & Li, W. 2000, *AJ*, 119, 2303
 Meikle, W. P. S., et al. 2007, *ApJ*, 665, 608
 Merrill, K. M. 1980, *IAU Circ.*, 3444, 1
 Miller, J. S., & Stone, R. P. S. 1993, *Lick Obs. Tech. Rep. 66* (Santa Cruz: Lick Obs.)
 Moffat, A. F. J., et al. 1998, *ApJ*, 497, 896
 Monnier, J. D., Tuthill, P. G., & Danchi, W. C. 1999, *ApJ*, 525, L97
 Monnier, J. D., Tuthill, P. G., & Danchi, W. C. 2002, *ApJ*, 567, L137
 Moseley, S. H., Dwek, E., Glaccum, W., Graham, J. R., Loewenstein, R. F., & Silverberg, R. F. 1989, *Nature*, 340, 697
 Nakano, S., Igataki, K., Puckett, T., & Gorelli, R. 2006, *CBET*, 666, 1
 Oke, J. B., et al. 1995, *PASP*, 107, 375
 Owocki, S. P. 2003, in *Massive Star Odyssey: From Main Sequence to Supernova*, ed. K. A. van der Hucht, A. Herrero, & C. Esteban (San Francisco: ASP), 281
 Pastorello, A., et al. 2007, *Nature*, 447, 829
 Smith, N. 2006, *ApJ*, 644, 1151
 Smith, N. 2007, *AJ*, 133, 1034
 Smith, N., & Conti, P. S. 2008, *ApJ*, in press
 Smith, N., & Gehrz, R. D. 2005, *AJ*, 129, 969
 Smith, N., & Owocki, S. P. 2006, *ApJ*, 645, L45
 Smith, N., et al. 2003, *AJ*, 125, 1458
 Smith, N., et al. 2007, *ApJ*, 666, 1116
 Sollerman, J., Leibundgut, B., & Spyromilio, J. 1998, *A&A*, 337, 207
 Stahl, O. 1986, *A&A*, 164, 321
 Stahl, O. 1987, *A&A*, 182, 229
 Stahl, O., et al. 1983, *A&A*, 127, 49
 Steiner, J. E., & Damini, A. 2004, *ApJ*, 612, L133
 Sugerman, B. E. K., et al. 2006, *Science*, 313, 196
 Temim, T., et al. 2006, *AJ*, 132, 1610
 Todini, P., & Ferrara, A. 2001, *MNRAS*, 325, 726
 Tuthill, P. G., Monnier, J. D., & Danchi, W. C. 1999, *Nature*, 398, 487
 Usov, V. V. 1999, *MNRAS*, 252, 49
 Van Dyk, S. D., Filippenko, A. V., & Li, W. 2002, *PASP*, 114, 700
 Wang, L., & Hu, J. 1994, *Nature*, 369, 380
 Wang, L., Wheeler, J. C., Kirshner, R. P., Challis, P. M., Filippenko, A. V., Fransson, C., Panagia, N., Phillips, M. M., & Suntzeff, N. 1996, *ApJ*, 466, 998
 Whitelock, P. A., Feast, M. W., Marang, F., & Breedt, E. 2004, *MNRAS*, 352, 447
 Wooden, D. H., Rank, D. M., Bregman, J. D., Witteborn, F. C., Tielens, A. G. G. M., Cohen, M., Pinto, P. A., & Axelrod, T. S. 1993, *ApJS*, 88, 477